Inorganic Chemistry

ARTICLE

pubs.acs.org/IC

Gold Nanoparticles Enhancing Dismutation of Superoxide Radical by Its Bis(dithiocarbamato)copper(II) Shell

Roberto Cao, Jr.,[†] Reynaldo Villalonga,[‡] Alicia M. Díaz-García,[†] Roberto Cao,*[,†] Teofilo Rojo,[§] and M. Carmen Rodríguez-Argüelles[∥]

[†]Lab. Bioinorgánica, Facultad de Química, Universidad de La Habana, Zapata y G, Vedado, La Habana 10400, Cuba

[‡]Departamento de Química Analitica, Facultad de Ciencias Químicas, Universidad Complutense de Madrid, 28040, Spain

[§]Departamento de Química Inorgánica, Facultad de Ciencias, Universidad del País Vasco, Apdo. 644, 48080 Bilbao, Spain

[∥]Departamento de Química Inorgánica, Universidade de Vigo, 36310 Vigo, Spain

Supporting Information

ABSTRACT: In the past few years three topics in nanoscience have received great attention: catalytic activity of gold nanoparticles (AuNPs), their electron transfer properties, and magnetism. Although these properties could have much in common no report on their synergism has been published. Here we present 10-nm gold nanoparticles conveniently capped with a mixed self-assembled monolayer containing bis(dithiocarbamato)copper(II) complexes, which dismutate superoxide radical with extremely high efficiency (IC_{50} = 0.074 μM). This behavior is interpreted as the result of an electron transfer (ET) process between AuNP core and the analyte when associated to copper(II). The ET process involving a charged AuNP core was detected by EPR and UV−vis spectroscopy.

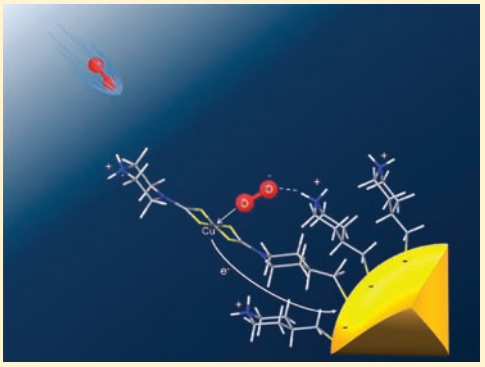

INTRODUCTION

Metal nanoparticles, MNPs, are receiving great attention in catalytic processes, in so-called nanocatalysis.[1,2] In this sense, special attention has been given to gold nanoparticles, AuNPs.[3] Apparently, the catalytic properties of AuNP depend on their unique electronic properties.[4] However, the catalytic properties of AuNP are only partially understood.[5] An approach to develop new types of nanocatalysts is to self-assemble metallic compounds on MNPs.[6,7] This way both the colloidal nature (extremely high surface area) of the nanoparticles and the known catalytic properties of coordination and organometallic compounds can be synergistically exploited.[8] The electronic properties of AuNPs allow them to capture/release electrons when interacting in redox reactions and thus could enhance the activity of an associated redox catalyst. Such consideration has not received sufficient attention until now despite the fact that AuNPs have been used as redox mediators in electrochemical biosensors.[9−11]

Very recently, the magnetic properties of AuNPs capped with thiolates have been studied. While bulk gold is diamagnetic, small AuNPs can present paramagnetism.[12,13]

A new challenge in nanocatalysis is to obtain MNPs capped with metal compounds which could mimic metalloenzymes. In this sense, it is important to mention that bis(dithiocarbamato)copper(II) ($CuDTC_2$) complexes have been studied as scavengers of superoxide anion to mimic Cu,Zn-superoxide dismutase (SOD).[14] When square planar $CuDTC_2$ dismutates superoxide anion, $O_2^{\bullet-}$, in a first step this radical is oxidized to O_2 while the complex is reduced to tetrahedral $CuDTC_2^{-}$.[15] Second, the $CuDTC_2^{-}$ is reoxidized by another $O_2^{\bullet-}$ that is reduced to hydrogen peroxide. This second step consumes two protons.

The active center of SOD corresponds to a strongly distorted planar copper(II). The channel that accesses this active site is provided with different positively charged amino acid residues, including Lys-120, Lys-134 (Figure 1a, indicated with arrows), and Arg-141 (Figure 1a, indicated with a star). In this sense, the presence of Arg-141 in a more internal location induces the final electrostatic attraction and fixes superoxide anion in a position favorable to coordinate to copper(II).[16]

Our main goal in this report was to obtain 10-nm AuNPs capped with four different highly stable asymmetric (two different dithiocarbamates) $CuDTC_2$ complexes (Scheme 1) able to present a significant SOD-like activity (dismutation of superoxide radical) enhanced by the AuNP core. Mixed monolayers of $CuDTC_2$ and 4-piperidinemethanethiolate, pipS, were also considered in the design.

RESULTS AND DISCUSSION

4-Piperidinemethanethioldithiocarbamate, DTCpipSH, provided the thiol group necessary to self-assemble the $CuDTC_2$

Received: August 31, 2010
Published: April 26, 2011

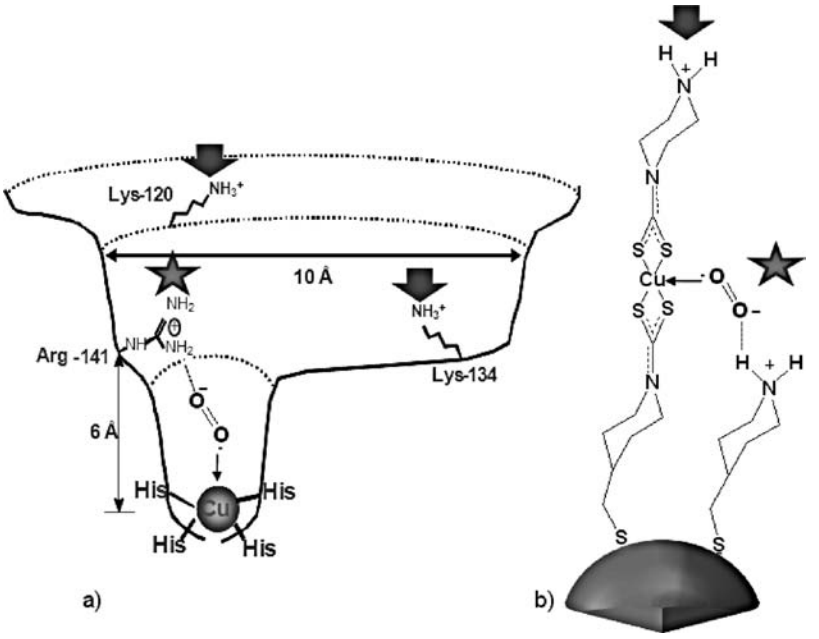

Figure 1. (a) Access cavity of Cu,Zn-SOD and (b) AuNP capped with mixed monolayer of asymmetric $CuDTC_2$ and pipS. Arrows and stars were used to indicate equivalences between the functional groups of parts a and b.

Scheme 1. Four Asymmetric $CuDTC_2$ Species Studied[a]

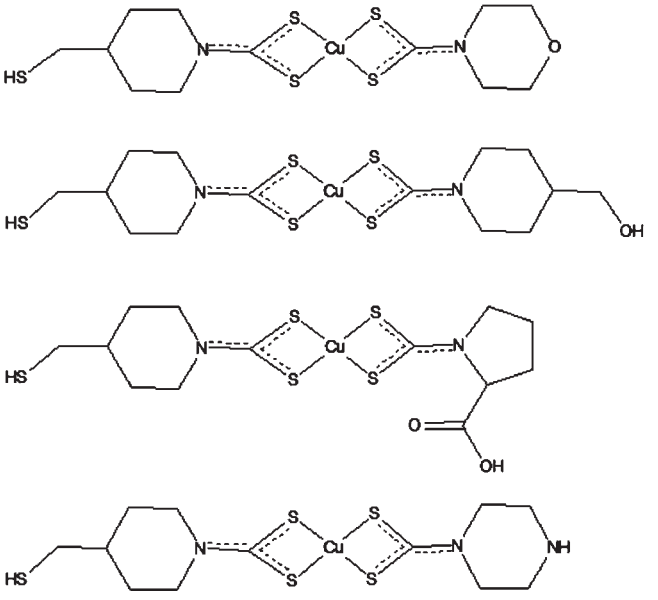

[a] From top to bottom: [Cu(DTCpipSH)(DTCmor)], [Cu(DTCpipSH)(DTCpipOH)], [Cu(DTCpipSH)(DTCpro)], and [Cu(DTCpipSH)(DTCpz)].

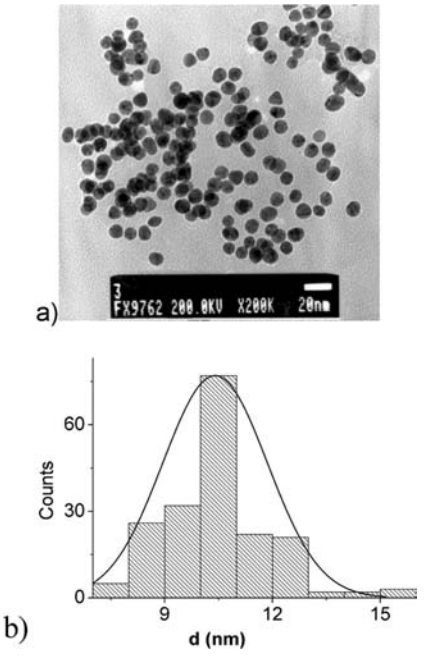

Figure 2. (a) TEM image of obtained AuNPs capped with citrate (bar scale 20 nm). (b) Size distribution of obtained AuNP-Cit.

complexes on AuNP and was synthesized as reported elsewhere.[17] The other dithiocarbamate ligands (morpholyldithiocarbamate, DTCmor; 4-piperidinomethanoldithiocarbamate, DTCpipOH; piperazinedithiocarbamate, DTCpz; and prolinedithiocarbamate, DTCpro), that complete the formation of the asymmetric $CuDTC_2$ complexes, present different terminal moieties.

Initially, four types of AuNP-$CuDTC_2$ nanoparticles were obtained by the interaction of each of the four $CuDTC_2$ complexes represented in Scheme 1 with AuNPs (capped with citrate),[18] with an average diameter of 10.4 (±1.2) nm (Figure 2). The AuNPs capped with citrate (AuNP-Cit) used presented the plasmon resonance maximum at 532 nm (Figure S1). AuNP-[Cu(DTCpipS)(DTCmor)] (**1**), AuNP-[Cu(DTCpipS)(DTCpipOH)] (**2**), AuNP-[Cu(DTCpipS)(DTCpro)] (**3**), and AuNP-[Cu(DTCpipS)(DTCpz)] (**4**) were designed in order to offer hydrophobic (**1**) and relatively hydrophilic (**2**, **3**, or **4**) surfaces. The hydrophilic nanoparticles were designed

dx.doi.org/10.1021/ic101770h |*Inorg. Chem.* 2011, 50, 4705–4712

Table 1. Composition (Obtained by XPS) and IC_{50} (μM) Values of the Different Types of Nanoparticles Studied

NP	% Cu	% S	% N	obtained Cu:S:N ratio (calcd)	μmol Cu/g NP	IC_{50} (μM of Cu)
1	3.80	18.52	7.34	1:4.89:1.93	26.2	18 (±2)
2	1.46	7.25	3.01	1:4.97:2.06 (1:5:2)	10.4	5.4 (±0.4)
2-pipS	1.51	8.17	3.97	1:5.41:2.63	10.9	4.5 (±0.5)
3	1.72	8.46	3.35	1:4.92:1.95(1:5:2)	12.4	7.6 (±0.8)
3-pipS	1.88	10.08	4.62	1:5.36:2.46	13.6	5.3 (±0.5)
4	3.20	15.81	9.70	1:4.94:3.03 (1:5:3)	23.1	2.3 (±0.2)
4-pipS$_1$	2.46	13.04	8.29	1:5.30:3.37	17.7	1.0 (±0.1)
4-pipS$_2$	1.87	10.71	7.10	1:5.72:3.79	13.5	0.24 (±0.01)
4-pipS$_3$	1.49	9.20	6.32	1:6.17:4.24	10.7	0.074 (±0.005)

with terminal groups that in physiological pH could generate neutral (**2**), negative (**3**), or positive (**4**) charges at their surfaces.

The four AuNP-$CuDTC_2$ systems, **1**−**4**, presented the IR, UV−vis, and EPR spectral characteristics of $CuDTC_2$ complexes. The maximum of the plasmon resonance of **1**−**4** laid around 545 nm (Figure S1). The expected shift in the plasmon maximum (from 532 nm) corresponds to the formation of the self-assembled monolayer that caps the nanoparticles. A maximum (mainly as a shoulder) around 432 nm, corresponding to $CuDTC_2$, was also recorded. These results indicate that $CuDTC_2$ did not decompose or modify its coordination mode upon the self-assembly process. Therefore, it may be concluded that the sulfur atoms of the DTC group have more affinity for copper(II) and less for the gold surface of AuNPs when compared with the thiol group of DTCpipS. This observation was previously reported by us.[17] Peaks at 162.26 and 163.46 eV in the XPS spectra confirmed the self-assembly of $CuDTC_2$ on AuNPs through the thiolate group of DTCpipS.[17] The peaks at 932.86 and 952.66 eV, corresponding to Cu 2p3/2 and 2p1/2, indicate that the metal is present as copper(II).

Once the four $CuDTC_2$ complexes were characterized their SOD-like activity was determined. This property is expressed as IC_{50}, the concentration of associated copper(II) necessary to inhibit in 50% enzymatically formed $O_2^{\bullet-}$.[19,20] Therefore, the lower the obtained IC_{50} values the higher the scavenging properties.

The determined SOD-like activity of the four $CuDTC_2$ complexes represented in Scheme 1 was low, with IC_{50} values between 1.2 and 8.8 μM, similar to that earlier reported for $Cu(DTCmor)_2$ (3.2 μM).[19] The SOD-like activity of nanoparticle **1** corresponded to IC_{50} of 18.0 μM. This value is extraordinarily higher than that for the native SOD (10^{-2}−10^{-3} μM),[16,21] and even than that for the free complex in solution, indicating a dramatically low catalytic activity. The high hydrophobic and compact shell of nanoparticle **1** (see amount of Cu in Table 1) should be the cause of this negative result. The SOD-like activity of the other three nanoparticles (**2**−**4**) was one order higher (Table 1). As expected, nanoparticle **4** presented the highest activity (2.32 μM). Nanoparticle **4**, with its positively charged terminal group (at physiological pH), was designed to mimic the function of Lys-120 and Lys-134. On the contrary, nanoparticle **3** (negatively charged surface) presented the lowest activity of these systems as was expected. These results speak about the importance of locating positive charges on the surface of the mimetic nanoparticles for the molecular recognition of $O_2^{\bullet-}$.

In order to favor the permeation of superoxide anion through the capping shell and access copper(II), a different type of mimetic was synthesized. In the new design the gold nanoparticles were capped with a mixed monolayer consisting of $CuDTC_2$ but also containing pipS as a second component (Figure 1b). The presence of pipS should not only provoke the necessary separation between the self-assembled $CuDTC_2$ complexes but also provide an inner secondary amino group (Figure 1b, indicated with a star) that could locate $O_2^{\bullet-}$ near to copper(II) through hydrogen bonds and electrostatic interactions (when protonated), mimicking Arg-141.

The IC_{50} values of nanoparticles **2**−**4** can be compared with those capped with the mixed monolayer formed by the corresponding $CuDTC_2$ and pipS (**2-pipS**, **3-pipS**, **4-pipS$_1$**, **4-pipS$_2$**, **4-pipS$_3$**) (Table 1). In all cases, the presence of pipS in the mixed monolayer enhanced the dismutation of $O_2^{\bullet-}$.

For the **4-pipS$_n$** system (with the lowest IC_{50} values) the surface composition was varied by modifying the $CuDTC_2$:pipS ratio in the mixed monolayer (Table 1). This way three types of nanoparticles, as that represented in Figure 1b, were obtained but differ in the composition of the capping shell. Note that the proportion of $CuDTC_2$ in the mixed monolayer dropped from **4-pipS$_1$** down to **4-pipS$_3$** as the IC_{50} value decreases.

The activity of **4-pipS$_3$** achieved a significant IC_{50} value of 0.074 μM. In other SOD mimics reported, where the presence of a positive charge next to copper(II) was considered in the design using quaternary ammonium,[20] and guanidinium moieties,[21] higher IC_{50} values (lower activity) were achieved. The presence of the inner protonated amino group (of pipS) favors the attraction of $O_2^{\bullet-}$ and H_2O, behaving as a mimetic of Arg-141 in the native enzyme (Figure 1a, indicated with a star). Nevertheless, this diffusion process should be less restricted in the case of free $CuDTC_2$ (in solution).

In order to support the important role played by pipS as a second short positively charged component in the mixed monolayer an additional experiment was performed. For this, nanoparticles similar to **4-pipS$_3$** were prepared but contain mercaptopropionate (MPA) instead of pipS in the capping shell. For such a system an IC_{50} value of 0.22 (±0.04) μM was obtained. Although the nanoparticles with MPA contained practically the same amount of copper (10.8 μmol Cu/g NP) as in **4-pipS$_3$** (10.7 μmol Cu/g NP) their SOD-like activity resulted in being one order lower than the latter.

Our interpretation on the extremely low IC_{50} value of **4-pipS$_3$** is that the AuNP core drives the redox reactions of the $CuDTC_2$ shell with $O_2^{\bullet-}$ through another pathway. As mentioned above, AuNPs can exchange electrons with electron donor or acceptor species. We believe that the achieved IC_{50} value of **4-pipS$_3$** is based on the consideration that the $CuDTC_2$ shell participates in

dx.doi.org/10.1021/ic101770h |*Inorg. Chem.* 2011, 50, 4705–4712

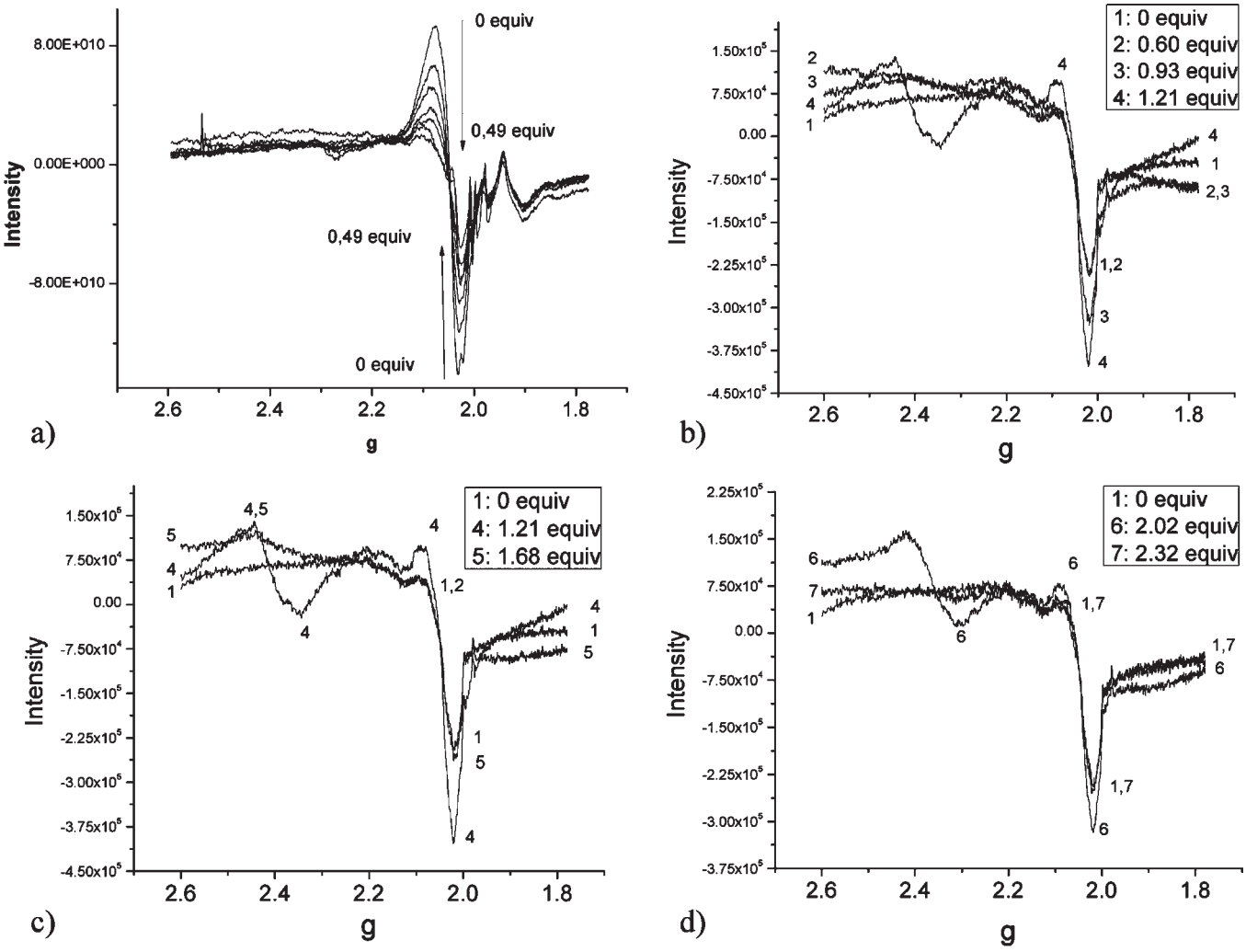

Figure 3. EPR spectra of the titration with KO_2 in *tert*-butanol (at RT) of (a) $[Cu(DTCpz)_2]$; (b) untreated **4-pipS$_3$** and after the first three additions of KO_2 (0.6−1.21 equiv.); (c) untreated **4-pipS$_3$** and after the addition of 1.21 and 1.68 equiv of KO_2, where the similarity between the first and third spectra can be observed; (d) untreated **4-pipS$_3$** and after the addition of 2.02 and 2.32 equiv of KO_2, where again similarities between the first and last spectra can be observed.

the attraction and coordination of the analyte and as a mediator in the redox process that could involve the AuNP core.

The reduction of the highly planar −N−CSS−Cu(II) group in $CuDTC_2$ involves a significant structural rearrangement in order to achieve its tetrahedral copper(I) complex.[14] On the other hand, $Cu(I)DTC_2^-$ and $O_2^{\bullet-}$ are both anions and should repel each other. Therefore, the cyclic redox reactions of $CuDTC_2$ with $O_2^{\bullet-}$ are not favored from electrostatic and conformational points of view.

In order to prove that an electron transfer (ET) process with the AuNP core took place, a specific electron paramagnetic resonance (EPR) experiment was designed and performed at room temperature (RT). A colloidal solution of **4-pipS$_3$** in *tert*-butanol was titrated with KO_2 (also dissolved in this solvent in the presence of 18-crown-6 ether) and followed by EPR. *tert*-Butanol was selected as solvent for three main reasons: (1) it is resistant to being oxidized by superoxide; (2) it is moderately polar and able to solvate superoxide anion; (3) as a tertiary alcohol it does not easily deprotonate. This latest characteristic restricts the possibility of reoxidation of $CuDTC_2^-$ (if formed) by superoxide anion, a reaction that is proton-dependent.

A control experiment was carried out using free $[Cu(DTCpz)_2]$ (not attached to AuNPs). The expected redox behavior (reduction) was observed by EPR spectra for the titration of free $[Cu(DTCpz)_2]$ with KO_2 (Figure 3a). The intensity of EPR signals of free $[Cu(DTCpz)_2]$ complex continuously decreased upon additions of KO_2 due to the reduction to $[Cu(DTCpz)_2]^-$, a diamagnetic species.

In the titration followed by EPR the first addition of superoxide solution (0.60 equiv of KO_2) to **4-pipS$_3$** did not affect the intensity of the paramagnetic signal (g = 2.06) of copper(II), but the second aliquot did (0.93 equiv) provoke its increment (Figure 3b). With the addition of 1.21 equiv of KO_2 the intensity of the peak at g = 2.06 continued to increase while a new one appeared at g = 2.41. The intensity of this latter peak did not vary within the first 20 min after the addition of the corresponding amount of KO_2 (Figure S2) which indicates that it does not correspond to an unstable intermediate species. We considered that the presence of the peak at g = 2.41 could be attributed to the formation of magnetic AuNPs. We also assumed that the copper-(II) signal at g = 2.06 could include a contribution of the magnetic AuNPs formed. Such an assumption would permit us

dx.doi.org/10.1021/ic101770h |*Inorg. Chem.* 2011, 50, 4705–4712

to explain the observed increase in the copper(II) peak at g = 2.06. The appearance of a new signal at g = 2.41 made us consider it due to the interaction of **4-pipS$_3$** with superoxide anion based on an ET process between the analyte and the AuNP core. When 1.68 equiv of KO_2 was added the signal at g = 2.41 practically disappeared completely, while that at g = 2.06 decreased in intensity but only down to the initial value (Figure 3c). The observed diminution in intensity of the signals at g = 2.41 and 2.06 should be associated with electron pairing in the magnetic AuNP core or the participation of the unpaired electron in the reduction of the analyte added. Further additions of KO_2 provoked the repetition of the already described variations in the EPR spectra (Figure 3d), but in this case the AuNP signal was shifted to g = 2.36. Such a shift is actually typical of ferromagnetic species, indicating that the electronic structure of the AuNP core is changing upon the ET process.

The intensity of the peak at g = 2.06 did not decrease (for additions of KO_2 up to 2.33 equiv) below its initial value signifying that the same amount of copper(II) was retained after the titration with KO_2 and that the observed variations in this signal are only due to the presence or not of unpaired electrons in the AuNP core.

The assignments made by us for the EPR peaks could be interpreted as is in contradiction with that reported before for small AuNPs capped with alkanethiols containing neutral terminal groups (−CH_3, −Ph) and not with positively charged moieties.[12] The reported paramagnetism of such small nanoparticles has been attributed to the formation of "holes" in the d level of AuNPs.[12,13] Evidently there are great differences between our system and the small AuNPs, but the assignments used served to interpret our observations. No earlier reports on magnetic studies of large AuNPs were found that would confirm our interpretations of the EPR spectra. Further studies will be required in order to offer a full interpretation on the observed magnetism of large AuNPs. We consider that the presence of a mixed monolayer capping AuNP could affect its electronic structure according to a recent report based on DFT calculations on AuNPs capped with mixed monolayers.[22] Even ferromagnetic 10-nm ZnO NPs capped with different organic molecules have been reported.[23]

In order to obtain additional experimental data that would support the proposed ET transfer to the AuNP core a titration of **4-pipS$_3$** with KO_2, under the same conditions as for the EPR determinations, was followed spectrophotometrically. Up to 2.92 equiv of KO_2 was added. A continuous increase in intensity of the plasmon resonance band was observed upon additions of KO_2, accompanied with a shift from 587 nm down to 575 nm (Figure 4). Both characteristics have been attributed to the storage of electrons in MNP cores.[24] The maximum at 587 nm indicates that a partial aggregation took place that could be influenced by the electrostatic interactions between the negative analyte and the positively charged **4-pipS$_3$**, especially when using *tert*-butanol. The results obtained by this experiment also support the consideration on the ET process involving the AuNP core.

With the aim of confirming that the size of **4-pipS$_3$** was not altered during the titration process, the resulting product was analyzed by TEM (Figure S3), and no significant variation in size was observed.

A control experiment was carried out in order to demonstrate that a AuNP itself can not dismutate superoxide anion. For this experiment AuNP was capped with cystamin in order to form a positively charged shell capable of attracting superoxide anion, but no dismutating activity was observed. Therefore, in the interaction of **4-pipS$_3$** with superoxide anion the presence of

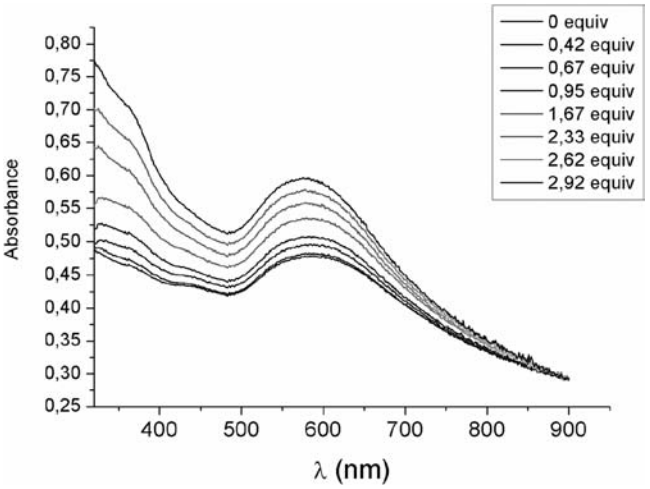

Figure 4. UV−vis spectra of the titration of **4-pipS$_3$** with KO_2. The maximum of the plasmon band shifted from 587 nm down to 575 nm while its intensity increased.

[Cu(DTCpipS)(DTCpz)] is indispensable and apparently behaves as a receptor of the analyte and as a redox mediator between it and the AuNP core, with the latter acting as an electron reservoir or "buffer". It is important to note that the redox processes of copper(II) take place at rates beyond the possibilities offered by common EPR or UV−vis determinations.

It is important to take into consideration that each electron captured by the AuNP core should attract counterions to its surface forming a double layer as in a capacitor (Figure 5).[12,25] The electron charge storage capacity per nanoparticle depends on the nanoparticle size (surface area) and its double-layer capacitance (C_{DL}), among other factors.

A 10-nm AuNP should not present a quantized double layer as in the case of smaller nanoparticles. We have considered that such a characteristic should not limit the ET process when the nanoparticle is interacting with superoxide anion.

As a consequence of the ET process an ionic double layer on the surface of the nanoparticle could be generated by the attraction of metallic cations and/or, according to the case, by the protonation of amino groups located at the surface of the nanoparticles, particularly for **4-pipS$_3$**. The attracted cations should not only tend to screen the negative charge of the electrons stored in the AuNP core, but also attract anions from the surroundings, including the analyte. This effect should mainly take place at low concentrations of the supporting electrolyte,[26] as used in our case (0.01 M).

C_{DL} depends directly on the dielectric constant of the mixed monolayer and inversely on its thickness. The presence of **pipS** as the second component of the mixed monolayer provides that certain zones of the shell are thinner, with a higher dielectric constant (smaller size, higher dipole moment). Thus, **4-pipS$_3$** should present the highest C_{DL} value and, therefore, the highest amount of stored electrons. In order to confirm this consideration an additional experiment was performed. The same titration with KO_2 followed by EPR was studied for **4-pipS$_1$** and **4-pipS$_2$** where a decrease in the g = 2.06 peak, below the initial value, was observed for very small aliquots of KO_2, of 0.17 equiv for **4-pipS$_1$** and 0.26 equiv for **4-pipS$_2$** (Figure S4). No peak at g = 2.41−2.36 was observed. Since the **4-pipS$_n$** system corresponds to nanoparticles with the same components, the differences in the redox

dx.doi.org/10.1021/ic101770h |*Inorg. Chem.* 2011, 50, 4705–4712

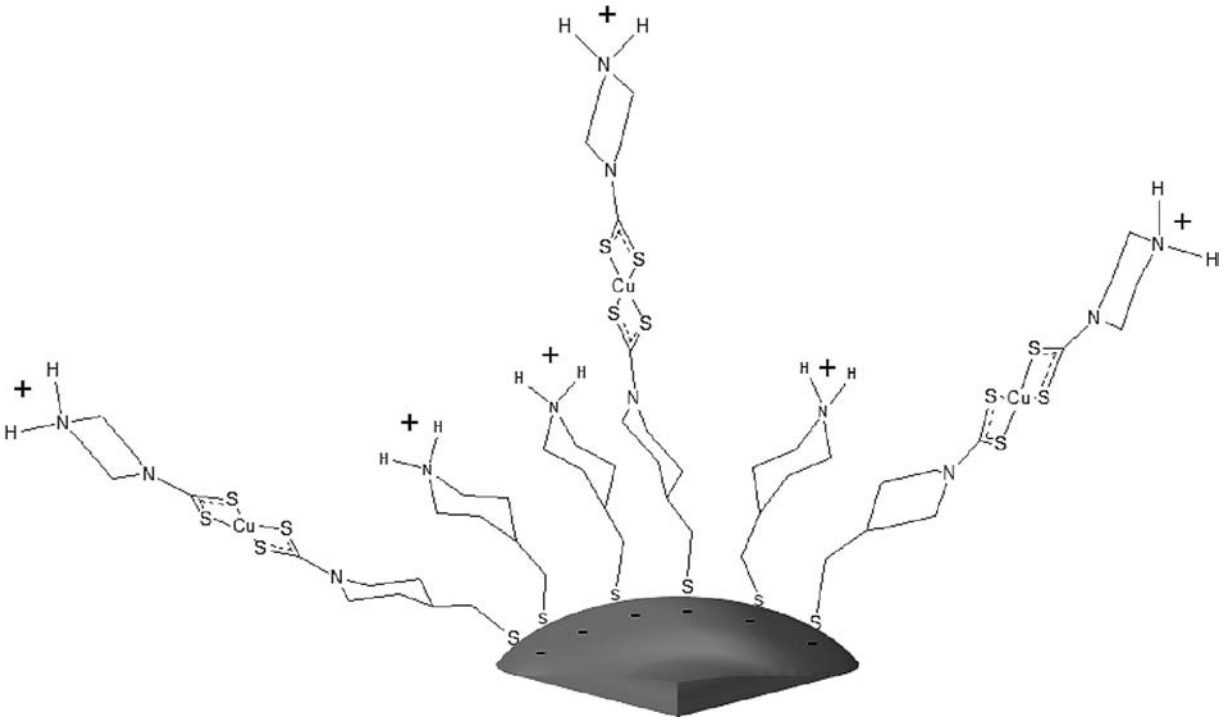

Figure 5. Scheme of the double layer formed by stored electrons in AuNP core and the protonated mixed monolayer.

behavior between them, when titrated with KO_2, should be attributed to the specific composition of the mixed monolayer, an important factor able to modulate C_{DL}.

Another positive influence of the formed double layer in the **4-pipS$_n$** system corresponds to the accumulation of vicinal protons which are necessary for the formation of hydrogen peroxide.

Summarizing, we consider that the enhanced efficiency of **4-pipS$_3$** is mainly due to a synergistic effect between each component of the nanoparticle: (a) the composition of the mixed monolayer containing protonated terminal and inner amino groups that assist the attraction and diffusion of the analyte, (b) the copper(II) center that coordinates $O_2^{\bullet-}$ and behaves as a redox mediator, and (c) the AuNP core acting as an electron reservoir with the best storage capacity.

The proposed pathway of the reaction involving the AuNP core should not only restrict the formation of negative $CuDTC_2^-$, which is electrostatically detrimental for the interaction with the analyte, but also contribute to the proton charging process at the surface of the nanoparticle via double layer formation.[27]

CONCLUSIONS

This paper probably constitutes the first report on the enhancing effect of AuNP cores on the catalytic properties of capping metal complexes. This effect has been attributed to an ET process between the analyte, when coordinated to copper(II), and the AuNP core. The EPR and UV−vis spectra recorded upon titration of **4-pipS$_3$** indicate that the AuNP core receives electrons from superoxide anion avoiding the unfavorable reduction of $CuDTC_2$. The electronic changes induced by ET processes involving large MNPs deserve further investigation.

An ET process, similar to that detected in **4-pipS$_3$**, could be present in other associated redox metal compounds in order to achieve an enhanced activity. The correct design of nanocatalysts based on MNPs capped with metal compounds is extremely important in order to observe an enhancement in the catalytic activity.

EXPERIMENTAL SECTION

Materials. Tetrachloroauric acid, 4-piperidinemethanol, and sodium sulfide were purchased from Aldrich, piperazine hexahydrate was purchased from Sigma, and the other chemicals were purchased from Merck. All reagents were of analytical grade and used without further purification. 4-Piperidinemethanethiol (pipSH) was synthesized as reported elsewhere.[17]

XPS. XPS measurements were performed using a VG Escalab 250 iXL ESCA instrument (VG Scientific), equipped with aluminum Al Kα monochromatized radiation at 1486.92 eV X-ray source. Photoelectrons were collected from a take off angle of 90° relative to the sample surface. The measurement was done in a constant analyzer energy mode (CAE) with a 100 eV pass energy for survey spectra and 20 eV pass energy for high resolution spectra. The binding scale was referenced by setting Au4f7/2 BE at 84.0 eV. Surface elemental composition was determined using the standard Scofield photoemission cross section method.

TEM. TEM determinations of AuNPs capped with citrate anions were carried out on a JEOL (2000FX model) microscope with a 200 kV acceleration voltage.

EPR. EPR measurements were performed on a Bruker EMX spectrometer (X-band, 9.5 GHz). Norell S-4-ERR-250S quartz tubes, with 3.0 mm internal diameter, were used. All measurements were carried out at 300 K. **4-pipS$_n$** (∼1.9 mg) was dispersed (by sonication) in dry *tert*-butanol (1 mL) for a copper concentration of 0.20 mM. Additionally, a solution of $[Cu(DTCpz)_2]$ (0.21 mM) was prepared, and another one of KO_2 (1 mM) with 18-crown-6 (10 mM) was prepared, both in dry *tert*-butanol. A 200 μL portion of each solution, **4-pipS$_n$** or $[Cu(DTCpz)_2]$, was introduced in EPR tubes and registered at 300 K. Aliquots of KO_2 (30 or 50 μL) were added to each solution, and the EPR was registered after each addition. The equipment parameters remained constant.

dx.doi.org/10.1021/ic101770h |*Inorg. Chem.* 2011, 50, 4705–4712

SOD-like Activity. The SOD-like activity was studied with the methodology previously described[19,20] using the xanthine−xanthine oxidase system to generate superoxide radical, phosphate buffer pH 7.0 (10 mM), nitroblue tetrazolium chloride (NBT) (2.5 μM), xanthine (10 μM), and the amount of xanthine oxidase required for slopes of ~0.025 Abs units/min. NBT reduction by superoxide radical was spectrophotometrically monitored at 560 nm. In the determination of the SOD-like activity of the different types of nanoparticles, it was necessary to control the concentration of $CuDTC_2$ capping AuNPs in each studied solution. For that, the molar amount of copper per milligram of nanoparticle was determined by XPS. About 2 mg of each type of nanoparticle was dispersed (by sonication) in water (1.5 mL), and then the concentration of $CuDTC_2$ in each solution was adjusted by dilution.

The percent of inhibition was calculated related to the slope of this first cuvette (ref slope) using the equation

$$\% \text{ inhibition} = (\text{assay slope-ref slope}) \times 100/\text{ref slope}$$

The IC_{50} values were determined by regression analysis and interpolation of the percent inhibition versus assay concentration curve, for no less than five experimental points for each system, with inhibition values within the range 10−75%. Inhibitions out of this range tend to have a nonlinear behavior. In all cases the linearity achieved was greater than 0.970.

Synthesis of the Asymmetric Bis(dithiocarbamato)copper(II) Complexes. 4-Piperidinemethanethiol (0.05 mmol) was mixed with the corresponding cyclic amine (4-piperidinemethanol, piperazine, proline or morpholine) in a pipSH:amine1:6 molar ratio in methanol with CS_2 (0.4 mmol) and ammonium (0.5 mL). To the resulting mixture was added a methanol solution of $CuCl_2$ (0.17 mmol) dropwise with constant stirring for 20 min, which was then rotory evaporated to dryness.

Synthesis of Gold Nanoparticles Capped with Citrate Anions. Gold nanoparticles capped with citrate anion (AuNP-Cit) were obtained using the procedure reported elsewhere.[18] A Na_3Cit:$AuCl_4^-$ = 7:1 molar ratio was used ($[AuCl_4^-]$ = 0.25 mmol). The reaction time at 100 °C was fixed for 30 min (under reflux). The resulting mother solution was stabilized with 0.01 M sodium dodecyl sulfate and was used to obtain the modified nanoparticles.

Synthesis of Gold Nanoparticles Capped with $CuDTC_2$ (1−4). To obtain nanoparticles **1**−**4** the corresponding asymmetric impure complex (45 mg of [Cu(DTCpipSH)(DTCmor)], 47 mg of [Cu(DTCpipSH)(DTCpipOH)], 53 mg of [Cu(DTCpipSH)(DTCprol)], or 45 mg of [Cu(DTCpipSH)(DTCpipNH)]) dissolved in DMSO (5 mL) was mixed with AuNP-Cit (40 mL) and stirred for 12−16 h. Ethanol (150 mL) was added and rotory evaporated to almost dryness. The resulting oil-like mixture was centrifuged (4000 rpm), and the obtained solids were washed with a DMSO:dioxane 2:1 mixture and centrifuged again. This process was repeated until the final liquid phase was completely colorless and free of AuNP (absence of Tyndall effect). The remaining solid was thoroughly washed with ethanol and ether and set to dry at RT.

Synthesis of Gold Nanoparticles Capped with a Mixed SAM of $CuDTC_2$ and pipS. A procedure similar to that mentioned above was used but with the additional presence of pipSH in a [Cu(DTCpipSH)(DTC)]:pipSH (2.4 mg) 1:1 molar ratio. For the nanoparticles containing [Cu(DTCpipSH)(DTCpz)] and pipS in the mixed monolayers, additional 1:10 (**4-pipS$_2$**) and 1:20 (**4-pipS$_3$**) molar ratios were also used.

■ ASSOCIATED CONTENT

Supporting Information. Figures S1 (UV−vis spectra of AuCit and nanoparticle **4**), S2 (EPR spectra vs time), S3 (TEM of **4-pipS$_3$** after titration with KO_2), and S4 (titration of **4-pipS$_2$** with KO_2 followed by EPR). This material is available free of charge via the Internet at http://pubs.acs.org.

■ AUTHOR INFORMATION

Corresponding Author

*E-mail: caov@fq.uh.cu. Phone: +537-8792145.

■ ACKNOWLEDGMENT

The authors acknowledge financial support from the University of Havana (Cuba), University of Matanzas (Cuba), and Spanish Ministry of Science and Innovation (CTQ2008-03059/PPQ), MAEC project A/031093/10, and are grateful to Prof. Dr. Nazario Martin and Dr. Emilio M. Pérez (IMDEA-Nano, Madrid, Spain) for valuable suggestions and to Dr. Carmen Serra (CACTI, Univ. Vigo, Spain) for XPS determinations. R.C., Jr., acknowledges scholarship from IMDEA-Nano (Madrid, Spain).

■ REFERENCES

(1) Astruc, D.; F. Lu, F.; Aranzaes, J. R. *Angew. Chem., Int. Ed.* **2005**, *44*, 7852–7872.
(2) Roucoux, A.; Schulz, J.; Patin, H. *Chem. Rev.* **2002**, *102*, 3757–3778.
(3) Chen, M.; Goodman, D. W. *Acc. Chem. Res.* **2006**, *39*, 739–746.
(4) Turner, M.; Golovko, V. B.; Vaughan, O. P. H.; Abdulkin, P.; Berenguer-Murcia, A.; Tikhov, M. S.; Johnson, B. F. G.; Lambert, R. M. *Nature* **2008**, *454*, 981–984.
(5) Grabow, L. C.; Mavrikakis, M. *Angew. Chem., Int. Ed.* **2008**, *47*, 2–5.
(6) Daniel, M. C.; Astruc, D. *Chem. Rev.* **2004**, *104*, 293–346.
(7) Wilton-Ely, J. D. E. T. *Dalton Trans.* **2008**, 25–29.
(8) Cao, R., Jr.; Díaz-García, A. M.; Cao, R. *Coord. Chem. Rev.* **2009**, *253*, 1262–1275.
(9) Villalonga, R.; Cao, R.; Fragoso, A. *Chem. Rev.* **2007**, *107*, 3088–3116.
(10) Villalonga, R.; Camacho, C.; Cao, R.; Hernández, J.; Matías, J. C. *Chem. Commun.* **2007**, 942–944.
(11) Baron, R.; Willner, B.; Willner, I. *Chem. Commun.* **2007**, 323–332.
(12) Zhu, M.; Aikens, C. M.; Hendrich, M. P.; Gupta, R.; Qian, H.; Schatz, G. C.; Jin, R. *J. Am. Chem. Soc.* **2009**, *131*, 2490–2492.
(13) Garitaonandia, J. S.; Insausti, M.; Goikolea, E.; Suzuki, M.; Cashion, J. D.; Kawamura, N.; Ohsawa, H.; Gil de Muro, I.; Suzuki, K.; Plazaola, F.; Rojo, T. *Nano Lett.* **2008**, *8*, 661–667.
(14) Cao, R.; Travieso, N.; Fragoso, A.; Villalonga, R.; Diaz, A.; Martinez, M. E.; Alpizar, J.; West, D. X. *J. Inorg. Biochem.* **1997**, *66*, 213–217.
(15) Christidis, P. C.; Georgousis, Z. D.; Hadjipavlou-Litina, D.; Bolos, C. A. *J. Mol. Struct.* **2008**, *872*, 73–80.
(16) Bertini, I.; Gray, H. B.; Lippard, S. J.; Valentine, J. S. *Bioinorganic Chemistry*; University Science Books: Mill Valley, CA, 1994; pp 298−304.
(17) Cao, R., Jr.; Díaz, A.; Cao, R.; Otero, A.; Cea, R.; Rodríguez-Argüelles, M. C.; Serra, C. *J. Am. Chem. Soc.* **2007**, *129*, 6927–6930.
(18) Ji, X.; Song, X.; Li, J.; Bai, Y.; Yang, W.; Peng, X. *J. Am. Chem. Soc.* **2007**, *129*, 13939–13948.
(19) Cao, R.; Fragoso, A.; Villalonga, R. *Monatsh. Chem.* **1996**, *127*, 775–782.
(20) Fragoso, A.; Cao, R.; D'Souza, V. T. *J. Carbohydr. Chem.* **1997**, *16*, 171–180.
(21) Fu, H.; Zhou, Y.-H.; Chen, W.-L.; Deqing, Z.-G.; Tong, M.-L.; Ji, L.-N.; Mao, Z.-W. *J. Am. Chem. Soc.* **2006**, *128*, 4924–4925.
(22) Rissner, F.; Egger, D. A.; Romaner, L.; Heimel, G.; Zojer, E. *ACS Nano* **2010**, *4*, 6735–6746.

(23) García, M. A.; Merino, J. M.; Fernández Pinel, E.; Quesada, A.; de la Venta, J.; Ruíz González, M. L.; Castro, G. R.; Crespo, P.; Llopis, J.; González-Calbet, J. M.; Hernando, A. *Nano Lett.* **2007**, *7*, 1489–1494.
(24) Hirakawa, T.; Kamat, P. V. *J. Am. Chem. Soc.* **2005**, *127*, 3929–3934.
(25) (a) Sardar, R.; Funston, A. M.; Mulvaney, P.; Murray, R. W. *Langmuir* **2009**, *25*, 13840–13851. (b) Murray, R. W. *Chem. Rev.* **2008**, *108*, 2688–2720.
(26) Hillier, A. C.; Kim, S.; Bard, A. J. *J. Phys. Chem.* **1996**, *100*, 18808–18817.
(27) Boettcher, S. W.; Berg, S. A.; Schierhorn, M.; Strandwitz, N. C.; Lonergan, M. C.; Stucky, G. D. *Nano Lett.* **2008**, *8*, 3404–3408.